Charge mobility determination by current extraction under linear increasing voltages: Case of nonequilibrium charges and field-dependent mobilities

Sebastian Bange,* Marcel Schubert, and Dieter Neher
Institut für Physik und Astronomie, Universität Potsdam, Karl-Liebknecht-Str. 24-25, 14476 Potsdam-Golm, Germany
(Received 3 July 2009; revised manuscript received 17 December 2009; published 26 January 2010)

The method of current extraction under linear increasing voltages (CELIV) allows for the simultaneous determination of charge mobilities and charge densities directly in thin-film geometries as used in organic photovoltaic (OPV) cells. It has been specifically applied to investigate the interrelation of microstructure and charge-transport properties in such systems. Numerical and analytical calculations presented in this work show that the evaluation of CELIV transients with the commonly used analysis scheme is error prone once charge recombination and, possibly, field-dependent charge mobilities are taken into account. The most important effects are an apparent time dependence of charge mobilities and errors in the determined field dependencies. Our results implicate that reports on time-dependent mobility relaxation in OPV materials obtained by the CELIV technique should be carefully revisited and confirmed by other measurement methods.

DOI: 10.1103/PhysRevB.81.035209 PACS number(s): 72.20.Jv, 72.40.+w, 72.80.Le

I. INTRODUCTION

The understanding of charge transport and recombination in thin layers of organic semiconducting materials is one of the keys for further improvement of optoelectronic devices such as organic light-emitting diodes and organic photovoltaic cells. Owned to it's simplicity, straightforward data analysis and applicability to measurements on films of well below 100 nm thickness, the technique of current extraction by linear increasing voltages (CELIV, see Ref. 1) has attracted considerable interest over the past years.[2–6] Its unique attractiveness stems from the opportunity to study charge transport directly in the thin-film geometries used in actual devices. As such, it became one of the main techniques to investigate structure-property relationships of charge transport and recombination in state-of-the-art donor/acceptor photovoltaic systems such as polymer/small molecule[7,8] and polymer/polymer[9] material blends, the morphology of which cannot be well reproduced in modified sample geometries or over a wide range of layer thicknesses. CELIV has originally been developed to determine charge mobility and concentration in microcrystalline Si:H semiconductors and doped conjugated polymers under thermal equilibrium conditions.[1,10] It was later applied to study the time and field dependences of the mobility of nonequilibrium charge carriers created by the absorption of a light pulse (photo-CELIV).[4,11,12] Hereby, a short (nanosecond) laser pulse generates a (if possible) homogeneous charge-carrier density throughout the active layer. After a given delay time, the external bias increases linearly, leading to the extraction of the photogenerated charge density from the layer. A rather general observation was that the charge-carrier mobility, as determined from the time of maximum extraction current, decays with increasing delay time.[3,6,8,9,13] This observation was attributed to the relaxation of carrier energies in an extended density of transport states and thus considered a sensitive parameter for device optimization. In fact, the Gaussian disorder model of charge transport in organic semiconductors predicts that after photoexcitation, charge carriers relax energetically toward their equilibrium energy, with a concomitant mobility decrease.[14] Additionally, charge mobilities and densities as determined by the photo-CELIV technique have been used to study the rate of nongeminate bimolecular charge recombination in organic solar cells, one of the loss factors for efficient generation of photocurrent.[3,4,13,15,16]

However, the analytic equations commonly used to evaluate CELIV experiments were derived by assuming a homogeneous density of *equilibrium* carriers. Deibel *et al.* recently pointed out that real devices exhibit an inhomogeneous distribution of electrons and holes in the device, with the electron concentration being highest at the cathode and lowest at the anode and vice versa for holes.[17] Numerical calculations showed that the spatial average of the recombination rate can be significantly lower in these cases than predicted for a homogeneous density of photogenerated electrons and holes. This effect might explain the common observation that Langevin-type recombination overestimates the decay of the carrier density with delay time in CELIV and similar charge-extraction experiments.[7,18–20]

Second, the illumination with a short laser pulse in the photo-CELIV experiment generates a nonequilibium carrier density, which shall be prone to bimolecular recombination before and during extraction. However, bimolecular charge recombination during extraction has not been taken into account in the analysis of the current transient.

This conceptual paper treats the analytic and numerical analysis of CELIV experiments under conditions diverging from the equilibrium assumptions of its original derivation. We first review the basic theory of equilibrium CELIV experiments and point out inaccuracies in the original derivations. Based on this, we treat the case of nonequilibrium photogenerated charge carriers with constant mobility by both numerical as well as analytical methods. We show that the equations typically used for data evaluation lead to an apparently time-dependent charge mobility, a feature that has been unanimously attributed to dispersive transport and the relaxation of charge carriers in an extended density of states. We provide an alternative analytic method to determine reliable values for charge mobilities under conditions of nonequilibrium charge-carrier recombination and discuss impli-

cations for experiments. Finally, we treat the application of CELIV measurements to the situation of field-dependent carrier mobilities. A modified analysis method is introduced and shown to result in significantly reduced errors for the derived field dependence.

II. CHARGE MOBILITY DETERMINATION BY THE CELIV TECHNIQUE

The experimental procedure and analytic evaluation for CELIV experiments has been introduced by Juška *et al.* in Ref. 1. Consider the extraction of equilibrium charge carriers of density n and mobility μ in the electric field U/d, where d is the layer thickness and $U(t)=U't$ is the applied voltage that rises linearly with time. Without restriction of the generality of our analysis, we assume that the internal electric field is zero at $U=0$. This differs from the more general situation where electrodes of different work functions are used. Experimentally, an external bias U_b is applied to compensate the built-in potential and ensure that the electric field within the organic layer is zero at $t=0$. As usual for the CELIV method, we assume that the electrode area A is much larger than d, that one carrier type is much more mobile than the other (here: holes), and that the electrodes are noninjecting under the chosen bias conditions. The time-dependent charge density is $\rho(z,t)=-en$ for $0\leq z\leq l(t)$ and $\rho(z,t)=0$ for $l(t)<z<d$. Thus, mobile holes are depleted from the layer up to the extraction depth $l(t)$. The current density measured in the external circuit due to the extraction of charges at $z=d$ is

$$j=\frac{\epsilon}{d}U'+\begin{cases}\dfrac{en}{d}\left(1-\dfrac{l}{d}\right)\left(\mu U't-\dfrac{en\mu l^2}{2\epsilon}\right) & [l(t)\leq d]\\ 0 & \text{else},\end{cases} \quad (1)$$

assuming $t\gg RC$, where R is the external circuit resistance and $C=\epsilon A/d$ is the geometrical sample capacitance assuming a permittivity of $\epsilon=\epsilon_r\epsilon_0$. The extraction depth is the solution of

$$\frac{dl(t)}{dt}+\frac{en\mu l^2(t)}{2d\epsilon}=\frac{\mu U't}{d} \quad (2)$$

under the initial conditions $l(0)=0$ and $dl(0)/dt=0$. This is a Ricatti-type nonlinear differential equation that can be solved numerically parametric in the dimensionless voltage slope $\epsilon^2U'/2e^2n^2\mu d^2$. At some time t_{max}, the current density [Eq. (1)] will peak at $j(t_{max})$, where the relative height $\Delta j/j=[j(t_{max})-j(0)]/j(0)$ can be expressed as a bijective function of the dimensionless parameter $\chi=\mu U't_{max}^2/2d^2$. Figure 1 shows the numerically calculated χ as a function of $\Delta j/j(0)$. χ is equal to 1/3 at $\Delta j/j(0)=0$ and decreases in a nonlinearly for $\Delta j/j(0)>0$. Also shown in Fig. 1 are two different parameterizations of this curve in terms of $\chi=\{3[1+0.18\Delta j/j(0)]\}^{-1}$ (fit I) and $\chi=0.329\exp[-0.180\Delta j/j(0)]+0.005\exp[0.253\Delta j/j(0)]$ (fit II) which are good approximations for $\Delta j/j(0)\leq 1$ or $\Delta j/j(0)\leq 7$ for fits I and fit II, respectively.

Using these, the charge mobility can be calculated from $\mu=2d^2\chi/U't_{max}^2$. This is in variance with the result published

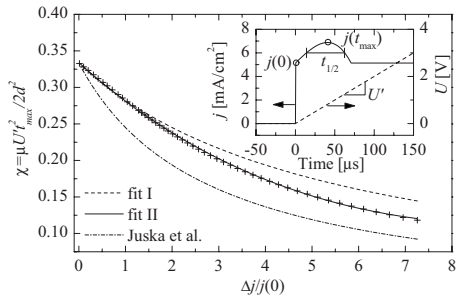

FIG. 1. Results of the calculation of χ as a function of $\Delta j/j(0)$ from the numerical solution of Eqs. (1) and (2) (symbols), compared to fits I and II as discussed in the text as well as the parameterization used by Juška *et al.* in Ref. 10. The inset shows a typical CELIV current calculated for $d=100$ nm, $U'=2\times10^4$ V/s, $\mu=2\times10^{-6}$ cm^2/V s, $n=10^{22}$ m^{-3}, $A=1$ mm^2, and $\epsilon_r=2.9$, indicating the capacitive charging current $j(0)$ and the maximum current $j(t_{max})$.

by Juška *et al.*[10,21] and used in several publications,[3,15,16] which corresponds to choosing $\chi=\{3[1+0.36\Delta j/j(0)]\}^{-1}$. In order to provide an independent test for the consistency of the presented results, we numerically simulated the CELIV experiment with a drift-diffusion solver assuming a typical charge mobility of $\mu=2\times10^{-6}$ cm^2/V s, a layer thickness of $d=65$ nm with $\epsilon_r=3$, a voltage slope of $U'=2\times10^4$ V/s, and an initial charge-carrier density of $n=4\times10^{22}$ m^{-3}. The numerically evaluated solution to Eqs. (1) and (2) closely reproduced the simulation results. We determined $\Delta j/j(0)=0.781$ and $t_{max}=25.125$ μs from the simulation data, from which the apparent mobilities $\mu=1.96\times10^{-6}$ cm^2/V s and $\mu=1.95\times10^{-6}$ cm^2/V s are calculated using fit I or II, respectively. Using the Juška *et al.* result, we instead obtain $\mu=1.74\times10^{-6}$ cm^2/V s, which proves that this approximation underestimates the mobility. Note that the relative error increases strongly in the experimentally convenient regime of large $\Delta j/j(0)$. We therefore suggest to calculate the CELIV mobilities using either of the new parameterizations, depending on the magnitude of $\Delta j/j(0)$. The inclusion of charge diffusion with a diffusion coefficient of $D=k_BT\mu/e$ lead to limited broadening but did not significantly alter the simulation results.

III. ROLE OF BIMOLECULAR CHARGE RECOMBINATION

Assuming charge recombination according to the Langevin mechanism,[22] the charge density at $z>l(t)$ decays as $n(t)=n(0)(1+t/\tau_\sigma)^{-1}$, where $\tau_\sigma=\epsilon/en(0)\mu$ is the dielectric relaxation time. This renders the evaluation of CELIV experiments as discussed above inaccurate and motivates to study the effects of charge recombination by numerical simulations. Figure 2 shows the results of numerically simulated current transients assuming $\mu=2\times10^{-6}$ cm^2/V s, $d=100$ nm, $\epsilon_r=3$, and $U'=2\times10^4$ V/s while varying the initial charge density $n(0)$ from 10^{22} to 10^{23} m^{-3}.

When bimolecular charge recombination is taken into account in the simulations, a significantly reduced amount of charges is extracted, reducing $\Delta j/j(0)$ and shifting t_{max} to-

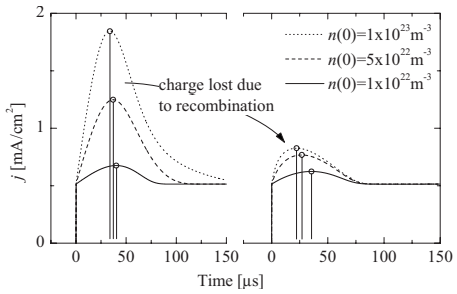

FIG. 2. Comparison of numerically simulated CELIV current transients without (left) and with (right) bimolecular charge recombination according to the Langevin mechanism, for simulation parameters see text. The results are shown parametric in the initial charge density and the position of $j(t_{max})$ is marked by a circle and vertical line.

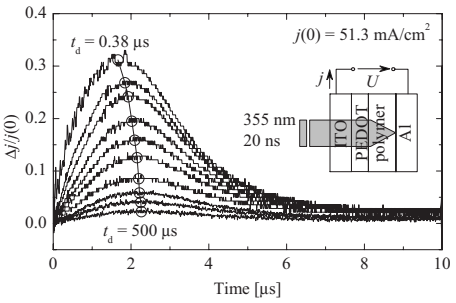

FIG. 3. Photo-CELIV current transients measured for a 55-nm-thick M3EH-PPV:CN-ether-PPV blend layer at $U'=1.06$ V/μs for different delay times after photoexcitation ranging from near zero up to 500 μs. Connected circles indicate the determined $j(t_{max})$ points. The inset schematically shows the layer structure and illumination direction used for the experiment.

ward shorter times. The apparent mobilities calculated from transients affected by recombination are expected to be higher compared to those calculated from recombination-free transients. We analyzed this in more detail for polymer blends of poly[2,5-dimethoxy-1,4-phenylenevinylene-2-methoxy-5-(2-ethylhexyloxy)-1,4-phenylenevinylene] (M3EH-PPV) with poly[oxa-1,4-phenylene-1,2-(1-cyano)-ethylene-2,5-dioctyloxy-1,4-phenylene-1,2-(2-cyano)-ethylene-1,4-phenylene] (CN-ether-PPV), for details of these materials see Ref. 9. Samples were fabricated by spincoating a 1:1 blend of these polymers from chlorobenzene solution (final layer thickness $d=55$ nm) onto precleaned and structured indium tin oxide (ITO) substrates covered by a layer of PEDOT:PSS (Clevios AI4083 obtained from H.C. Starck, Germany) and evaporating a 200-nm-thick aluminum top electrode. The active electrode area was $A=4$ mm^2 to ensure a short RC time of approximately 100 ns. Devices were fabricated under protective nitrogen atmosphere and encapsulated by a cover glass and two-component epoxy resin prior to measurements under ambient conditions. Charge carriers were photoexcited with 20 ns long pulses of 355 nm wavelength and a fluence of 3.54 J/m^2 while biasing the ITO electrode at 0.63 V positive with respect to the aluminum electrode to cancel the internal electric field and avoid premature charge extraction. Figure 3 shows photo-CELIV current transients obtained at a voltage slope of $U'=1.06$ V/μs for various delay times t_d between photogeneration and the beginning of charge extraction.

Note that the extraction voltage pulse was applied in reverse direction to avoid charge injection from the electrodes as verified by a purely capacitive response in case of missing photoexcitation. As is obvious from the current transients, the time t_{max} of maximum extraction current strongly shifts to smaller values for short t_d. We simulated the current transients taking into account Langevin-type recombination, with the model parameters $d=55$ nm, $U'=1.06$ V/μs, and $\epsilon=3$ and using a field-independent and time-independent mobility $\mu=3.8\times10^{-6}$ cm^2/V s as observed in the limit of long delays. The initial charge density is difficult to directly determine experimentally since the photogeneration of free carriers is a function of the local electric field and the donor/acceptor blend microstructure. An upper bound for the generation efficiency is given by the incident photon to converted electron efficiency of $\eta_{IPCE}=0.2$ as measured under short circuit conditions. The active layer typically absorbs around 60% of the incident radiation at the laser wavelength and thus we estimate that an upper bound to the generated charge density $n(0)$ at the beginning of the extraction pulse is 7×10^{24} m^{-3}. Since the actual charge density might be significantly lower, it was varied between 10^{21} and 10^{25} m^{-3} for the simulations. Figure 4 shows the $\Delta j/j(0)$ and apparent mobilities calculated from simulated photo-CELIV transients.

The apparent mobility (solid symbols) rises with charge density for $n(0)>10^{23}$ m^{-3}, corresponding to current maxima (open symbols) of $\Delta j/j(0)>0.1$. It has been suggested[23] that CELIV transients are most convenient to determine experimentally when $\Delta j/j(0)\approx1$. Our simulations discourage this choice for the investigation of nonequilibrium charge carriers since charge recombination strongly distorts the transients in this regime. In a next step, the delay time t_d between photogeneration of charge carriers of density n_{photo} and charge extraction was varied, whereby the charge density at the beginning of charge extraction is

$$n(t_d)=n_{photo}/(1+e\mu n_{photo}t_d/\epsilon). \quad (3)$$

Figure 5 compares the apparent mobilities calculated from simulation data with experimental values obtained from Fig. 3.

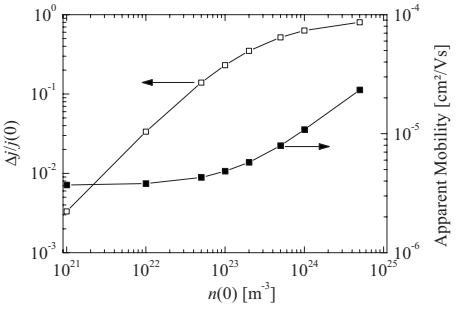

FIG. 4. Analysis of numerically simulated CELIV transients in terms of current maximum $\Delta j/j(0)$ (open symbols) and apparent mobility (solid symbols, calculated using *chi* from fit II) for a range of charge densities $n(0)$ present at the beginning of charge extraction ($t_d=0$). The simulation model parameters correspond to the experimental situation of Fig. 3.

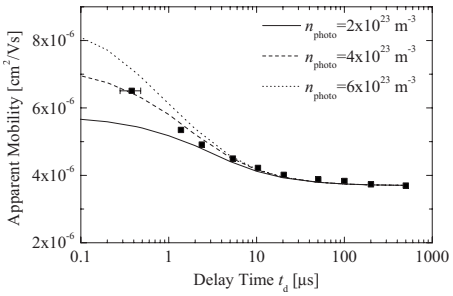

FIG. 5. Apparent mobility calculated from Fig. 3 (filled symbols, using χ from fit II), compared to numerical simulations (lines) assuming various initial charge-carrier densities n_{photo}, a time-independent charge mobility $\mu=3.8\times10^{-6}$ cm^2/V s, and Langevin-type charge recombination. Data is shown as a function of the delay time t_d between photoexcitation and the beginning of the extraction voltage pulse, the approximate uncertainty of the delay time for the first data point is indicated by the error bar.

Assuming $n_{\text{photo}}=4\times10^{23}$ m^{-3}, simulated results closely follow those obtained experimentally over the whole range of delay times investigated. For the shortest delay time in the experiment ($t_d=0.38$ μs) our simulations predict an extracted carrier density of 5×10^{22} m^{-3}, which is in excellent agreement with the value determined in the actual experiment. The comparison to the density $n(t_d)$ of 3×10^{23} m^{-3} according to Eq. (3) shows, that a significant fraction of carrier density present at $t=t_d$ recombines during extraction.

In order to quantify the effect of charge recombination and to provide a guideline for CELIV experiments under nonequilibrium conditions, we discuss an analytic treatment of the situation. In general, the charge density ρ will follow complicated spatial and time dependences since charge recombination will take place only in the region $z>l(t)$, where both charge types are present. To keep our analysis sufficiently general, we limit it to the case of bimolecular charge recombination, considering a dielectric relaxation time given by $\tau_\sigma=\epsilon/en(0)\mu\beta$, where β is a recombination prefactor ($\beta=1$ corresponds to Langevin recombination). Reduced bimolecular recombination with $\beta\ll1$ has been shown to prevail in some polymer/small molecule donor/acceptor blend solar-cell materials.[7,19,20] Most of these report use photo-CELIV or similar techniques to determine time-dependent charge densities and mobilities. In photo-CELIV, the spatial charge distribution for $z\leq l(t)$ depends on $l(t)$ as

$$\rho(z)=\frac{-en_0}{1+\tau_\sigma^{-1}l^{(-1)}(z)}, \tag{4}$$

where $l[l^{(-1)}(z)]=z$ defines the inverse function $l^{(-1)}(z)$ of $l(t)$. Despite this implicit expression for the charge density, analysis shows that the current transient can be obtained by the surprisingly simple expression

$$j=\frac{\epsilon}{d}U'+en\frac{1-l/d}{1+t/\tau_\sigma}\frac{dl(t)}{dt}. \tag{5}$$

The time dependence of $l(t)$ is calculated from

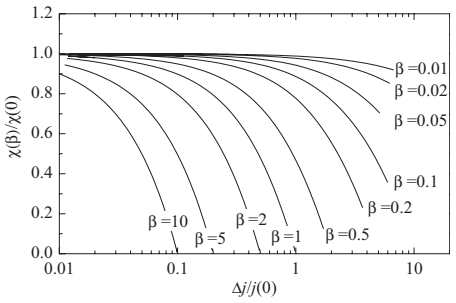

FIG. 6. Results of the calculation of $\chi(\beta)/\chi(0)$ as a function of $\Delta j/j(0)$ from the numerical solution of Eqs. (5) and (6), parametric in the bimolecular recombination prefactor β.

$$\frac{d^2l(t)}{dt^2}=\frac{\mu U'}{d}-\frac{1}{d\beta\tau_\sigma}\frac{l(t)}{1+t/\tau_\sigma}\frac{dl(t)}{dt}, \tag{6}$$

the solution of which converges to that of Eq. (2) for $\beta\to0$. We compared this solution to the results of numerical simulations and found good agreement when charge diffusion was neglected in the simulations. Using the same techniques as for Fig. 1, we calculated χ as a function of $\Delta j/j(0)$ parametric in the prefactor β. Figure 6 plots the results relative to χ as determined for $\beta=0$.

Given a specific recombination prefactor β, these curves can be used to directly extract the recombination-corrected charge mobility from the measurement or to estimate the impact of recombination on CELIV results obtained by simple analysis discussed earlier. We additionally fitted χ as a function of $\Delta j/j(0)$ for the case $\beta=1$ by the double exponential expression corresponding to fit II. This directly results in the expression

$$\mu=\frac{2d^2}{U't_{\max}^2}(0.860e^{-0.486\Delta j/j(0)}-0.525e^{0.0077\Delta j/j(0)}) \tag{7}$$

which is valid at $\Delta j/j(0)<0.95$ with a relative error of less than 3.5% and can be used to determine true charge mobilities from CELIV transients even under conditions of high charge densities, assuming that Langevin recombination prevails.

We further analyze the ratio of extraction current peak's half width $t_{1/2}$ to the peak position $t_{\max}$, see Fig. 1. This ratio has been used as a dispersion parameter, where an increase in $t_{1/2}/t_{\max}$ at short delay times after photogeneration was interpreted in terms of a dispersive charge transport as expected for disordered transport systems shortly after photogeneration.[15,16] Figure 7 shows this parameter as a function of $\Delta j/j(0)$ parametric in β.

Juška *et al.*[15] pointed out that this parameter equals 1.2 under conditions of time-independent charge mobilities but this is obviously only true for $\Delta j/j(0)\to0$. Similar to $\chi(\beta)/\chi(0)$, it diverges at finite values of $\Delta j/j(0)$. Values significantly larger than 1.2 are obtained even for $\beta\to0$ due to a distortion of the current transient by the formation of space charges during extraction.

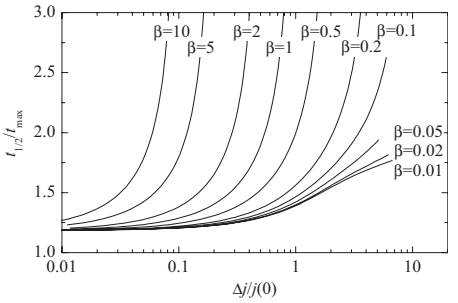

FIG. 7. The transport dispersion parameter $t_{1/2}/t_{\max}$ as a function of $\Delta j/j(0)$, parametric in the bimolecular recombination prefactor β.

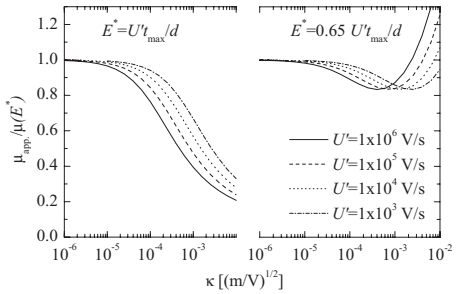

FIG. 8. Ratio of the apparent mobility $\mu_{\text{app.}}$ and the actual mobility at the electric field of $E^*=U't_{\max}/d$ (left) and $E^*=0.65U't_{\max}/d$ (right) as a function of the Poole-Frenkel parameter κ. The apparent mobility was calculated from the current transients given by Eq. (8) using $\mu_0=10^{-6}$ cm^2/V s, $d=100$ nm, and $\epsilon_r=3$ as well as using χ from fit I and is shown parametric in the voltage slope U'.

IV. FIELD-DEPENDENT CHARGE MOBILITIES

The charge mobility in organic semiconductors is usually considered to be both a field-dependent and a density-dependent quantity, where the electric field dependence has been experimentally found to mostly follow a Poole-Frenkel-type law $\mu(E)=\mu_0 \exp(\kappa\sqrt{E})$ in a field range typically assessed in CELIV experiments.[14] The work of Bässler *et al.* has shown that this can be understood in terms of transport sites having random energies according to a Gaussian distribution, rendering μ_0 and κ temperature dependent.[24] CELIV experiments provide a unique opportunity to determine charge mobilities in undoped organic semiconductor films of well below 100 nm thickness but has the disadvantage of working under conditions of a nonconstant electric field. Since the mobility is calculated from the maximum extraction current point, the determined values have usually been associated with the electric field $E^*=U't_{\max}/d$ (*extraction field*) present at the time of maximum extraction current,[2,4,13] although the validity of this approach has never been tested rigorously. As we have shown above, mobilities determined for nonequilibrium charge carriers using photo-CELIV are more reliable when $\Delta j/j(0)\ll 1$, i.e., when $\tau_\sigma \gg t_{\text{tr}}$, where $t_{\text{tr}}=d\sqrt{2/\mu U'}$ is the charge transit time through the layer. Under this approximation, the current density [Eq. (1)] becomes

$$j=\frac{\epsilon}{d}U'+\frac{en}{d}\left(1-\frac{l}{d}\right)U't\mu_0 e^{\kappa^*} \tag{8}$$

for $l(t)\leq d$, where

$$l(t)=\frac{2\mu_0}{U'\kappa^4}[6d+6de^{\kappa^*}(\kappa^*-1)+U't\kappa^2 e^{\kappa^*}(\kappa^*-3)] \tag{9}$$

and $\kappa^*(t)=\kappa\sqrt{U't/d}$. Unfortunately, Eq. (8) does not provide any closed analytic expression for $t_{\max}$ and $\Delta j/j(0)$ but can be evaluated numerically. Figure 8 compares the apparent charge mobility calculated from such data using χ (fit I) to the actual mobility at $E=E^*=U't_{\max}/d$.

These results were calculated for $\mu_0=10^{-6}$ cm^2/V s, $d=100$ nm, and $\epsilon_r=3$ but are considered to be fairly general since they are independent of n at sufficiently low densities and invariant under the mutual transformation $\mu_0\rightarrow\alpha\mu_0$, $U'\rightarrow\alpha U'$ for arbitrary α. It is obvious that significant errors in the apparent mobility occur at large κ and large U'. We propose a simple improvement of the CELIV analysis by attributing the apparent mobility values to the extraction field redefined as $E^*=0.65U't_{\max}/d$. The corresponding relative error of the apparent mobility is also shown in Fig. 8 and stays within 20% in the relevant parameter regime. In order to test this approach, we numerically simulated CELIV transients in the $\Delta j/j(0)\ll 1$ regime for various values of U', assuming $d=100$ nm, $\epsilon_r=3$, $\mu_0=10^{-6}$ cm^2/V s, and $\kappa=10^{-3}$ (m/V)$^{1/2}$. Figure 9 compares the apparent mobility values determined using χ from fit I, associated with either choice of E^*.

We found that using $E^*=0.65U't_{\max}/d$ generally gives better results for this type of field dependence. The experimental error can be further minimized by using an iterative procedure if the field dependence of the apparent mobility indeed follows the Poole-Frenkel behavior: (1) measure CELIV transients at different U' to obtain a range of $t_{\max}$ and μ values, (2) determine preliminary parameters $\mu_0^{(0)}$ and $\kappa^{(0)}$ from the measurement using $E^*=U't_{\max}/d$, (3) for each U', calculate the theoretical CELIV transient from Eq. (8), numerically evaluate $[\Delta j/j(0)]^{\text{th}}$, $t_{\max}^{\text{th}}$, and μ^{th} using $\mu^{\text{th}}=2d^2\chi/U'(t_{\max}^{\text{th}})^2$ and calculate $\delta=d\ln(\mu^{\text{th}}/\mu_0^{(0)})/U't_{\max}^{\text{th}}\kappa^{(0)}$, (4) associate each *measured* mobility value to the extraction field $E^*=\delta U't_{\max}/d$ and determine optimized $\mu_0^{(1)}$ and $\kappa^{(1)}$

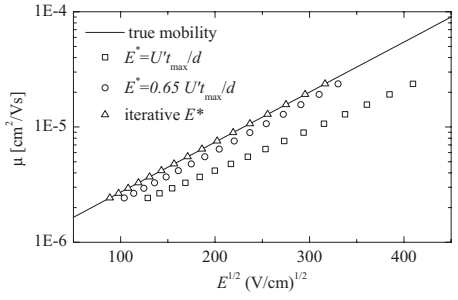

FIG. 9. Apparent charge mobilities calculated from simulated CELIV transients using χ from fit I for field-dependent charge mobilities as indicated by the solid line. The extraction field associated to determined mobility values was calculated as $E^*=U't_{\max}/d$ (squares), $E^*=0.65U't_{\max}/d$ (circles), or using the iterative procedure as described in the text (triangles).

from this data, and (5) iterate the procedure by repeating steps 3 and 4 until the determined $\mu_0^{(n)}$ and $\kappa^{(n)}$ stabilize. This procedure is only moderately complex but significantly enhances the accuracy of charge mobility determination, at least when Poole-Frenkel field dependence prevails. Figure 9 shows that the results of this iteration procedure accurately track the true field-dependent mobility used for the simulated CELIV experiments.

V. CONCLUSION

In this paper, we pointed out several difficulties that arise when applying the photo-CELIV technique under realistic conditions usually encountered in experiments. We based our analysis upon a rederivation of the original CELIV analysis, correcting for inaccuracies in the original publications that result in erroneous charge mobilities under conditions of high charge density. In the case of photogenerated charge carriers, we found a significant departure from the equilibrium assumption of the original derivations. The impact of bimolecular charge recombination during extraction on CELIV transients and their analysis in this situation has not been considered up to now. We showed that high charge densities as typically used in the experiments can lead to an artificial time dependence of the determined mobility values. We were able to relate the experimental results for a M3EH-PPV/CN-ether-PPV blend solar cell to this effect, showing that it is possible to explain the experimental results with a reasonable initial charge density and a charge mobility that is constant in time. Information was provided to facilitate an interpretation of experiments under conditions of nonequilibrium charge-carrier extraction. We further analyzed the relative width of the CELIV current peak that has been used in the past to characterize transport dispersion expected for charge carriers energetically relaxing in a broad density of states. $t_{1/2}/t_{\max}$ as measured by the photo-CELIV technique under conditions of non-negligible $\Delta j/j(0)$ was shown to be inadequate to assess the transport dispersion of photogenerated charge carriers due to it's inherent connection to charge-recombination and space-charge effects. As another deviation from idealized conditions we investigated the effect of field-dependent charge-carrier mobilities. We showed that association of the CELIV mobilities with the electric field present at the time of extraction current maximum leads to significant errors in the determined field dependence. An optimized choice of the correlated extraction field was introduced, which yields much lower errors compared to the standard approach. Additionally, we showed that under the presumption of a Poole-Frenkel-type field dependence, an iterative procedure can be applied to determine the true mobility-field dependence.

We note that the presented analytic treatment for photo-CELIV experiments is still strongly simplified in that it does not take into account bipolar transport or spatial inhomogeneities in the initial charge distributions. As pointed out recently by Deibel *et al.*,[17] the assumption of spatial homogeneous charge densities leads to further errors in CELIV results that also contribute to an apparently reduced recombination prefactor β. In conclusion, the photo-CELIV method, owed to it's inherent spatial and time-averaging properties, fails to provide unambiguous insight into photogenerated charge-carrier dynamics.

ACKNOWLEDGMENTS

S.B. acknowledges financial support by the German Federal Ministry of Science and Education (BMBF under Grants No. FKZ 13N8953 and No. 03X3525D). M.Sch. acknowledges financial support by the German Research Foundation (DFG) SPP 1355.

*Present address: University of Utah, Department of Physics and Astronomy, 115 South 1400 East #201, Salt Lake City, UT 84112-0830, USA; sbange@physics.utah.edu

[1] G. Juska, K. Arlauskas, M. Viliunas, and J. Kocka, Phys. Rev. Lett. **84**, 4946 (2000).
[2] G. Juska, K. Genevicius, K. Arlauskas, R. Osterbacka, and H. Stubb, Phys. Rev. B **65**, 233208 (2002).
[3] R. Österbacka, A. Pivrikas, G. Juska, K. Genevicius, K. Arlauskas, and H. Stubb, Curr. Appl. Phys. **4**, 534 (2004).
[4] A. J. Mozer, N. S. Sariciftci, A. Pivrikas, R. Österbacka, G. Juska, L. Brassat, and H. Bässler, Phys. Rev. B **71**, 035214 (2005).
[5] G. Dennler, A. J. Mozer, G. Juska, A. Pivrikas, R. Österbacka, A. Fuchsbauer, and N. S. Sariciftci, Org. Electron. **7**, 229 (2006).
[6] B. Homa, M. Andersson, and O. Inganas, Org. Electron. **10**, 501 (2009).
[7] A. Pivrikas, N. S. Sariciftci, G. Juska, and R. Österbacka, Prog. Photovoltaics **15**, 677 (2007).
[8] M. Schubert, C. Yin, M. Castellani, S. Bange, T. L. Tam, A. Sellinger, H.-H. Hörhold, T. Kietzke, and D. Neher, J. Chem. Phys. **130**, 094703 (2009).
[9] C. Yin, M. Schubert, S. Bange, B. Stiller, M. Castellani, D. Neher, M. Kumke, and H. H. Hörhold, J. Phys. Chem. C **112**, 14607 (2008).
[10] G. Juska, K. Arlauskas, M. Viliunas, K. Genevicius, R. Österbacka, and H. Stubb, Phys. Rev. B **62**, R16235 (2000).
[11] G. Juska, K. Genevicius, R. Österbacka, K. Arlauskas, T. Kreouzis, D. D. C. Bradley, and H. Stubb, Phys. Rev. B **67**, 081201(R) (2003).
[12] K. Genevicius, R. Österbacka, G. Juska, K. Arlauskas, and H. Stubb, Synth. Met. **137**, 1407 (2003).
[13] A. J. Mozer, G. Dennler, N. S. Sariciftci, M. Westerling, A. Pivrikas, R. Österbacka, and G. Juska, Phys. Rev. B **72**, 035217 (2005).
[14] D. Hertel and H. Bässler, ChemPhysChem **9**, 666 (2008).
[15] G. Juska, N. Nekrasas, K. Genevicius, J. Stuchlik, and J. Kocka, Thin Solid Films **451-452**, 290 (2004).
[16] A. J. Mozer, N. S. Sariciftci, L. Lutsen, D. Vanderzande, R. Österbacka, M. Westerling, and G. Juska, Appl. Phys. Lett. **86**,

112104 (2005).
[17] C. Deibel, A. Wagenpfahl, and V. Dyakonov, Phys. Rev. B **80**, 075203 (2009).
[18] A. Pivrikas, G. Juska, A. J. Mozer, M. Scharber, K. Arlauskas, N. S. Sariciftci, H. Stubb, and R. Osterbacka, Phys. Rev. Lett. **94**, 176806 (2005).
[19] G. Juska, K. Arlauskas, J. Stuchlik, and R. Österbacka, J. Non-Cryst. Solids **352**, 1167 (2006).
[20] C. Deibel, A. Baumann, and V. Dyakonov, Appl. Phys. Lett. **93**, 163303 (2008).
[21] G. Juska, M. Viliunas, K. Arlauskas, N. Nekrasas, N. Wyrsch, and L. Feitknecht, J. Appl. Phys. **89**, 4971 (2001).
[22] P. Langevin, Ann. Chim. Phys. **28**, 433 (1903).
[23] K. Genevicius, R. Österbacka, G. Juska, K. Arlauskas, and H. Stubb, Thin Solid Films **403-404**, 415 (2002).
[24] H. Bässler, Phys. Status Solidi B **175**, 15 (1993).